

1963

The gamma fission cross section of thorium-232 near threshold

Harlan Duwaynne Dulmage
The University of Montana

Let us know how access to this document benefits you.

Follow this and additional works at: <https://scholarworks.umt.edu/etd>

Recommended Citation

Dulmage, Harlan Duwaynne, "The gamma fission cross section of thorium-232 near threshold" (1963). *Graduate Student Theses, Dissertations, & Professional Papers*. 8308.
<https://scholarworks.umt.edu/etd/8308>

This Thesis is brought to you for free and open access by the Graduate School at ScholarWorks at University of Montana. It has been accepted for inclusion in Graduate Student Theses, Dissertations, & Professional Papers by an authorized administrator of ScholarWorks at University of Montana. For more information, please contact scholarworks@mso.umt.edu.

THE GAMMA FISSION CROSS SECTION
OF THORIUM-232 NEAR THRESHOLD

by

HARLAN DUWAYNNE DULMAGE

B.S. Northwestern University, 1960


Presented in partial fulfillment of the requirements
for the degree of


Master of Arts

MONTANA STATE UNIVERSITY

1963

Approved by:


Chairman, Board of Examiners


Dean, Graduate School

JUN 24 1963

Date

UMI Number: EP39109

All rights reserved

INFORMATION TO ALL USERS

The quality of this reproduction is dependent upon the quality of the copy submitted.

In the unlikely event that the author did not send a complete manuscript and there are missing pages, these will be noted. Also, if material had to be removed, a note will indicate the deletion.



UMI EP39109

Published by ProQuest LLC (2013). Copyright in the Dissertation held by the Author.

Microform Edition © ProQuest LLC.

All rights reserved. This work is protected against unauthorized copying under Title 17, United States Code



ProQuest LLC.
789 East Eisenhower Parkway
P.O. Box 1346
Ann Arbor, MI 48106 - 1346

ACKNOWLEDGEMENTS

I am deeply grateful to Doctor Mark J. Jakobson for his assistance in suggesting this work and in guiding me throughout the investigation.

For help in constructing the target chamber and in operating the linear accelerator I would like to thank David L. Browman, William R. Ellis, John T. Hoven and Robert O. Vosburgh.

TABLE OF CONTENTS

	page
Introduction	1
Experimental Procedure and Equipment	3
Measurement procedure	3
Targets	4
Catcher foils	4
Counter	7
Incident beam	7
Results	8
Conclusions	24
References	26

INTRODUCTION

Nuclear fission has been investigated quite extensively. An early model, the liquid drop model¹, made it possible to present a picture of some of the mechanisms of nuclear fission. A later replacement, the collective model², allowed additional treatment for dependency on independent particles. This model added to theory the probability that fission will occur by barrier penetration. The relative probability of a nuclear reaction is measured by the nuclear cross section. The cross section for a reaction may be thought of as the cross sectional area, or target area, presented by a nucleus to an incident particle.

For fission by photons, (γ, f), current theory leads one to expect a relatively regular dependence of fission cross section upon photon energy. Cross sections for neighboring heavy nuclei with even numbers of protons and even numbers of neutrons are also expected to be similar. Furthermore, theory leads one to expect that the (γ, f) cross section for a nuclide will decrease after the threshold of a competing reaction such as the (γ, n) reaction, due to competition between the two reactions. Therefore a decrease should appear in the fission cross section (σ_f) just after the (γ, n) threshold. Experiments by Katz et al.³

have shown this to be the case. The research of Katz and co-workers indicated that there is also a decrease in (γ, f) for Th^{232} below the (γ, n) threshold. If these measurements are correct, the decrease in the cross section is not explained by present theory. Also, these measurements indicate no corresponding decrease in σ_f for U^{238} which would be expected. The question of the true existence of this decrease in Th^{232} , and of the lack of a similar one in the σ_f of U^{238} , led to the investigation described in this thesis.

EXPERIMENTAL PROCEDURE and EQUIPMENT

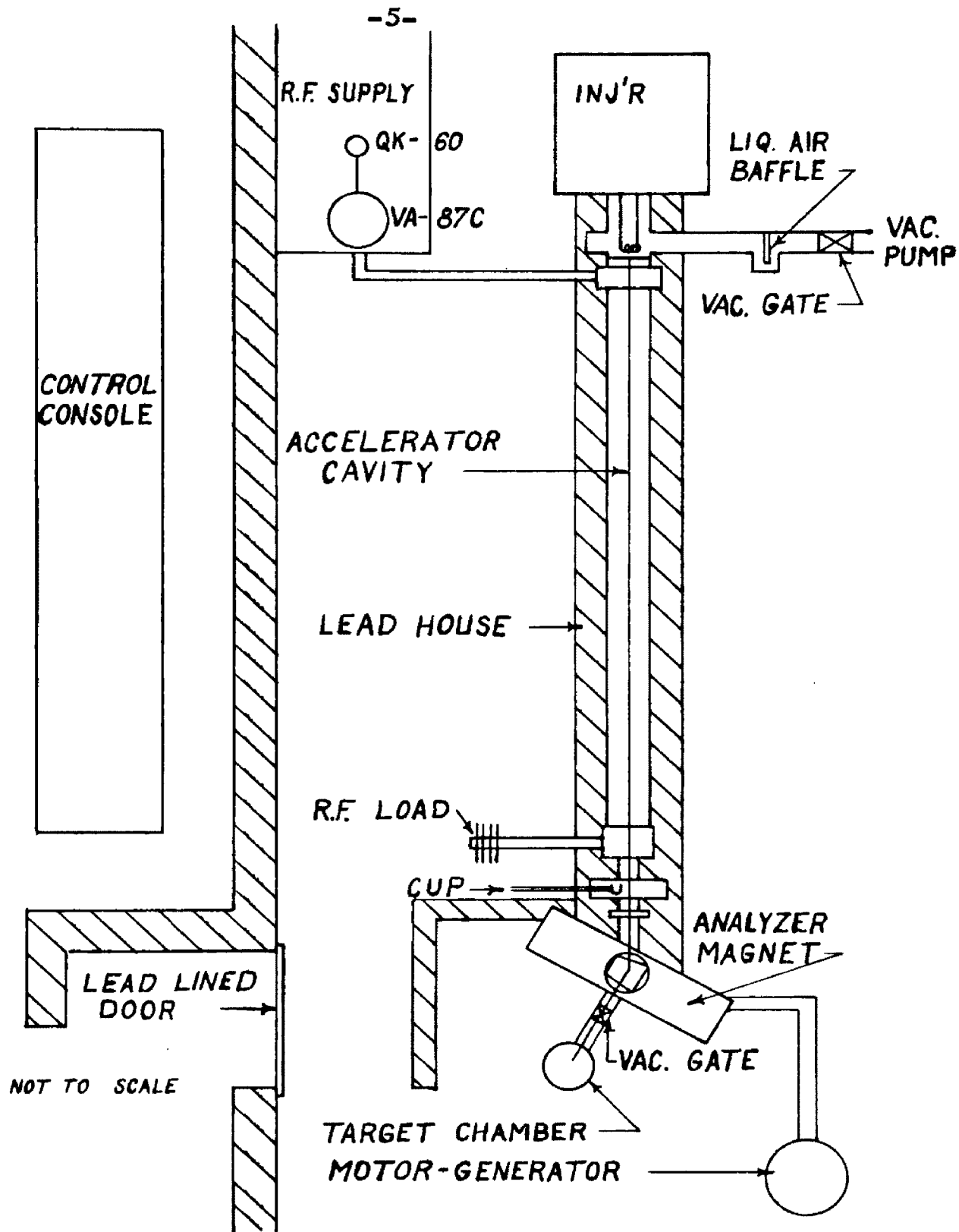
The relative number of fissions caused by incident photons were measured by counting the radioactivity of the fission fragments. An aluminum catcher foil, placed near the target, was used to catch the fission fragments. Then the beta activity of these fission fragments was measured, using a geiger counter. The assumption was made that the beta activity would be proportional to the number of fission fragments and that their activity would not change for the energy range involved. This assumption was checked by seeing that the fission fragment half lives at the different energy levels did not change appreciably.

Measurement procedure- The general arrangement in the laboratory is shown in Fig. 1 with the target chamber an integral part of the accelerator vacuum system. A catcher foil was placed in position in the target chamber. After the chamber was evacuated by a mechanical pump it was connected to the linear accelerator by opening the gate at the exit of the analyzer magnet. The time to evacuate the chamber to a pressure such that the accelerator could be operated averaged about six minutes. The target was radiated for a period of ten minutes with a beam of approximately 0.1μ amperes and the catcher foil removed from the chamber. AS soon

as possible the catcher foil was placed in position below the window of the geiger counter and the number of counts were recorded at 1, 2, 4, 6, 8, 10, 12, and 15 minute intervals from the beginning of the counting period. The counts at these different times were taken in order to check the half lives of the fission fragments. The activity graphs and cross section calculations are based upon total counts for ten minutes.

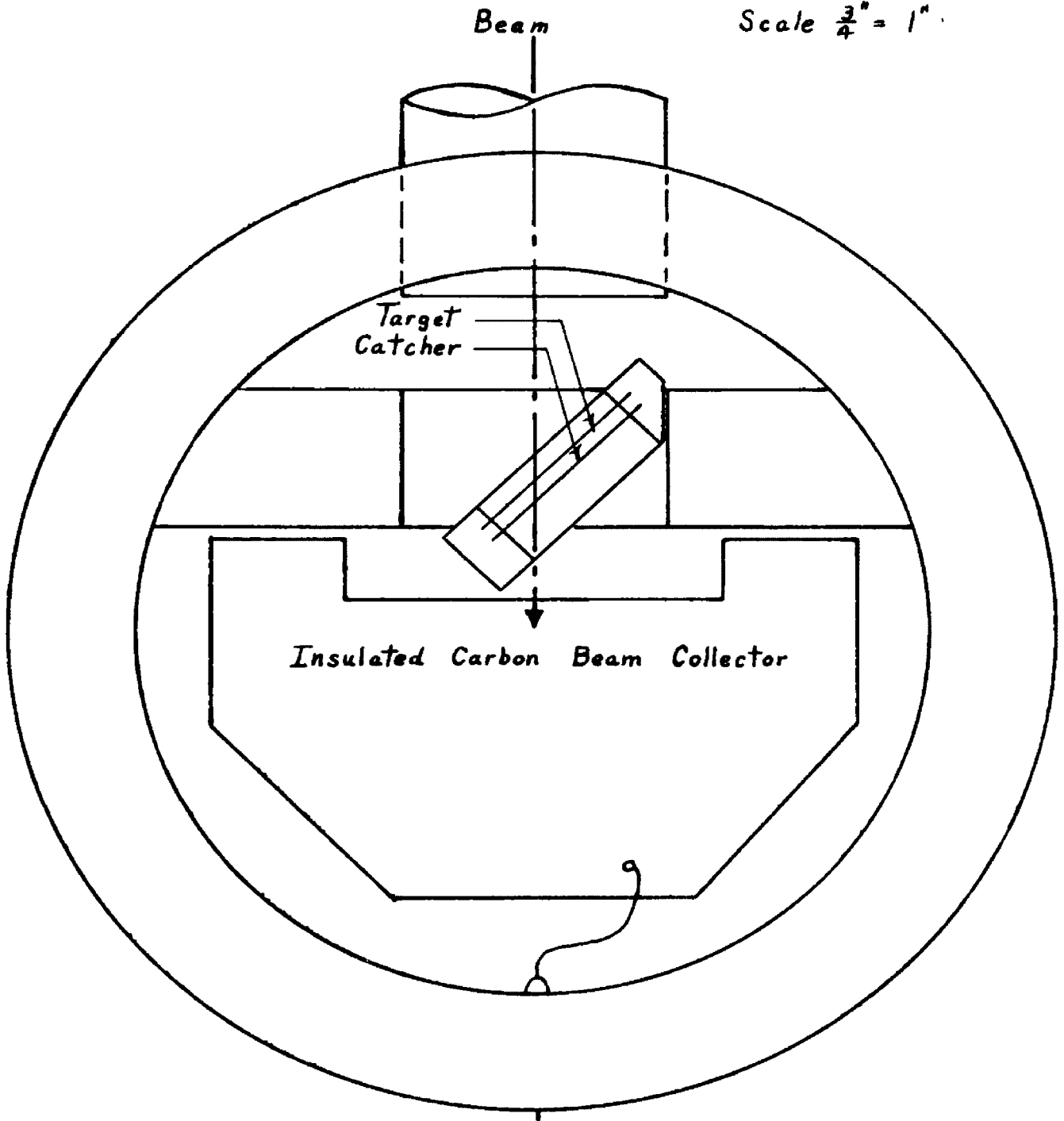
Targets- One and one half inch squares of foil 0.0015" and 0.002" thick of Th^{232} and U^{238} respectively were used as targets in the experiment. Brass foil was overlapped 1/8" on the sides and bottom of the targets for purposes of making them more rigid. The targets were positioned 45° to the beam as shown in Fig. 2. The beam, 1/2" high, covered a band crossing the center of the target. The sides of the holder were low enough so that only the target was in the beam path.

Catcher foils- Aluminum foil (0.001" thick) and aluminum sheeting (1/16" thick) were used as catchers during the experiment. The catcher foils used for most of the runs were made of aluminum foil of double thickness. The mean range in air of light fission fragments⁴ has been measured to be 2.65 cm.; this is essentially the maximum range of the fragments since range straggle is not appreciable. The range in air has a corresponding range in aluminum of 0.0005", thus the catcher foils were thick



MONTANA STATE UNIVERSITY
 LINEAR ACCELERATOR LAYOUT
 Fig. 1

Scale $\frac{3}{4}'' = 1''$



EVACUATED TARGET CHAMBER

Fig. 2

enough to stop essentially all fragments. The shape of the catcher foils was rectangular, approximately 2" x 1.5" in each case. The corners were folded back allowing each catcher foil to fit into a 2" diameter circle.

Counter- The geiger counter used in the experiment was a 2" diameter beta detector, the AC-2 OMNI/GUARD counter manufactured by Tracerlab Inc. The detector is actually two geiger tubes, a guard tube surrounding all but the bottom surface of the counting tube. This system uses the guard and counting tubes and a coincident circuit so that only radiation which does not have a coincident pulse in the guard tube is counted from the counting tube. The background count is reduced from about 20 cpm to one cpm by this system.

Incident beam- Monoenergetic electrons were obtained from the Montana State University linear accelerator⁵. For energies 5.45 Mev and below the beam was 0.2 μ amp., and for 5.50 Mev and above the beam was 0.1 μ amp.

RESULTS

The relative activities of the fission products for the different energies are shown in Figs. 3 and 4. The counts are normalized for a 35 second delay, which occurred from the time the beam was turned off to the beginning of the counting period. The actual time delay varied from 25 to 35 seconds with a few delays being of the order of 40 seconds. The normalization was done by use of an average decay curve for the counting period. This decay curve (Fig. 5) was fitted to the average counts per minute of thorium for the ten electron energies from 5.55 Mev to 6.00 Mev. The points designated by horizontal lines are either coincident or too close to another point to be able to designate them clearly. A check showed that the thorium curve fit the decrease in the activity of the uranium fission fragments. Therefore, the thorium curve was used to normalize all runs for thorium and uranium.

The activity per incident electron that would be induced in a sample after an infinitely long irradiation⁶ is

$$\alpha(E_0) = ec \int_0^{E_0} \sigma(k) P(k, E_0) dk,$$

where $\sigma(k)$ is the cross section for photon energy k and $P(k, E_0)$ is the number of photons per Mev per incident

electron produced in the photon energy interval k to $k + dk$ for an electron energy E_0 . The constant e is the detection efficiency and c is the number of nuclei per cm^2 . An approximation to the above equation is made by summing over a series of energy intervals of width ϵ and average cross section ($\bar{\sigma}$) for the interval,

$$\alpha(E_0) = ec \sum_n \bar{\sigma}[E_0 - (n + \frac{1}{2})\epsilon] P[E_0 - (n + \frac{1}{2})\epsilon, E_0],$$

where $n = 0, 1, 2, \dots, \frac{E_0}{\epsilon} - 1$. $P(k, E_0)$ is expressed in units of photons per ϵ Mev interval per incident electron. This equation when solved for the average cross section may be rewritten as

$$\bar{\sigma}(E_0 - \frac{1}{2}\epsilon) = \Delta A(E_0) - \sum_k \bar{\sigma}(k) \Delta\phi(k, E_0)$$

where $k = \frac{\epsilon}{2}, \frac{3}{2}\epsilon, \dots, E_0 - \frac{3}{2}\epsilon$,

$$\text{and } \Delta A(E_0) = \frac{1}{ec} \frac{\alpha(E_0) - \alpha(E_0 - \epsilon)}{P(E_0 - \frac{1}{2}\epsilon, E_0)}$$

$$\text{and } \Delta\phi(k, E_0) = \frac{P(k, E_0) - P(k, E_0 - \epsilon)}{P(E_0 - \frac{1}{2}\epsilon, E_0)}$$

The values of $P(k, E_0)$ are obtained from the corrected Sauter-Fano curves⁷ of the bremsstrahlung spectrum of electrons. Fig. 6 represents the curves obtained when the assumption is made that $P(k, E_0)$ is a linear function from 5.0 Mev to 6.0 Mev for values of k from 5.025 Mev to 5.975 Mev. The shape of the

plotted Sauter-Fano curves indicate that this is a reasonable approximation. Fig. 6 indicates the number of photons $P(k, E_0)$ produced with energy k to $k + \epsilon$ for electron energy E_0 .

Using the $P(k, E_0)$ vs E_0 graph (Fig. 6) the values of $\Delta\phi(k, E_0)$ are calculated as indicated in the equation for $\Delta\phi(k, E_0)$. The value of $\Delta\phi(k, E_0)$ is constant over the range of k because of the linear assumption made to obtain the $P(k, E_0)$ vs E_0 curves. $\Delta\phi(k, E_0)$ is not constant for different values of ϵ since $P(k, E_0)$ is a function of ϵ . Curves for $\epsilon = 0.1$ Mev and $\epsilon = 0.05$ Mev are given in Figs. 7 and 8. As is seen $\Delta\phi(k, E_0)$ has a larger value for $\epsilon = 0.1$ Mev than for $\epsilon = 0.05$ Mev. This is understandable because there are more photons per energy interval when the energy interval is increased. The curves rather than the calculated points are employed in calculating the cross section.

The final relative values of the cross sections are given in Figs. 9 to 12. Fig. 9 for thorium shows the standard deviation only and Fig. 10 shows the combined standard deviation and statistical error due to the photon difference method. The curves for U^{238} are plotted similarly (Figs. 11 & 12).

The error shown in the relative activity figures is the standard deviation obtained from the uncorrected total counts at that energy. Because of this error

designated $st[\alpha(E_0)]$ there is a statistical error $st[\bar{\sigma}(k)]$ in the calculation of the cross section. If $st[\alpha(E_0)]$ does not vary much for neighboring values of E_0 , a good approximation of the statistical error⁸ is

$$st[\bar{\sigma}(k)] = \frac{1}{\epsilon^{3/2}} E_0 st[\alpha(E_0)] \cdot \text{constant.}$$

The constant may be evaluated by the equation

$$\bar{\sigma}(k) = \frac{1}{\epsilon} \sum_n C_{k,n} \alpha(E_{0n})$$

where $n = \frac{\epsilon}{2}, \frac{3}{2}\epsilon, \dots, k$. The value of $\alpha(E_{0n})$ used in the evaluation is 5.3 Mev with $k = 5.275$ Mev for Th^{232} and 5.4 Mev with $k = 5.35$ Mev for U^{238} . The constant in the statistical error equation is the $C_{k,n}$ for the first cross section computed.

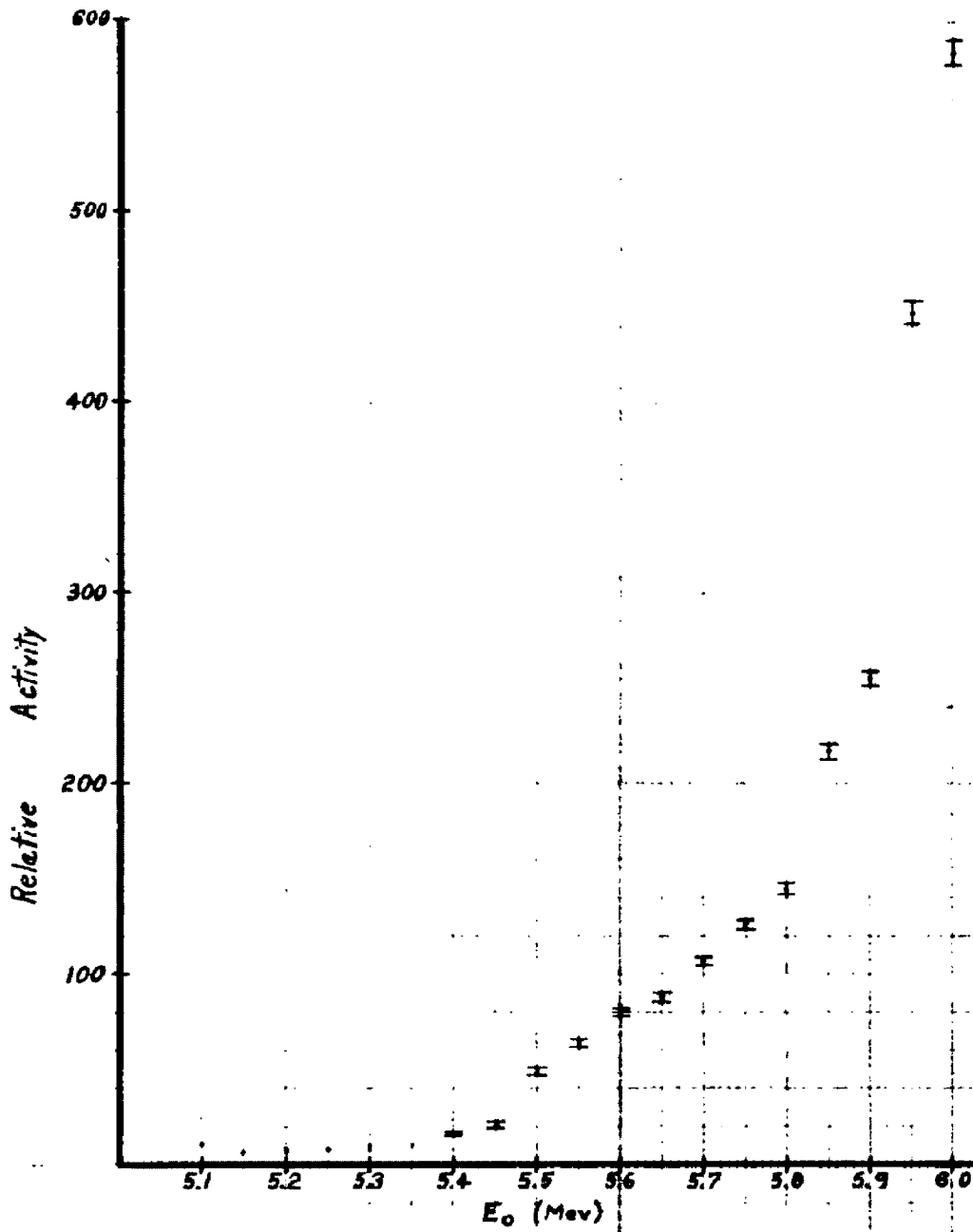


Fig. 3 Activity of Fission Particles from Th^{232} for Electron Energy E_0 .

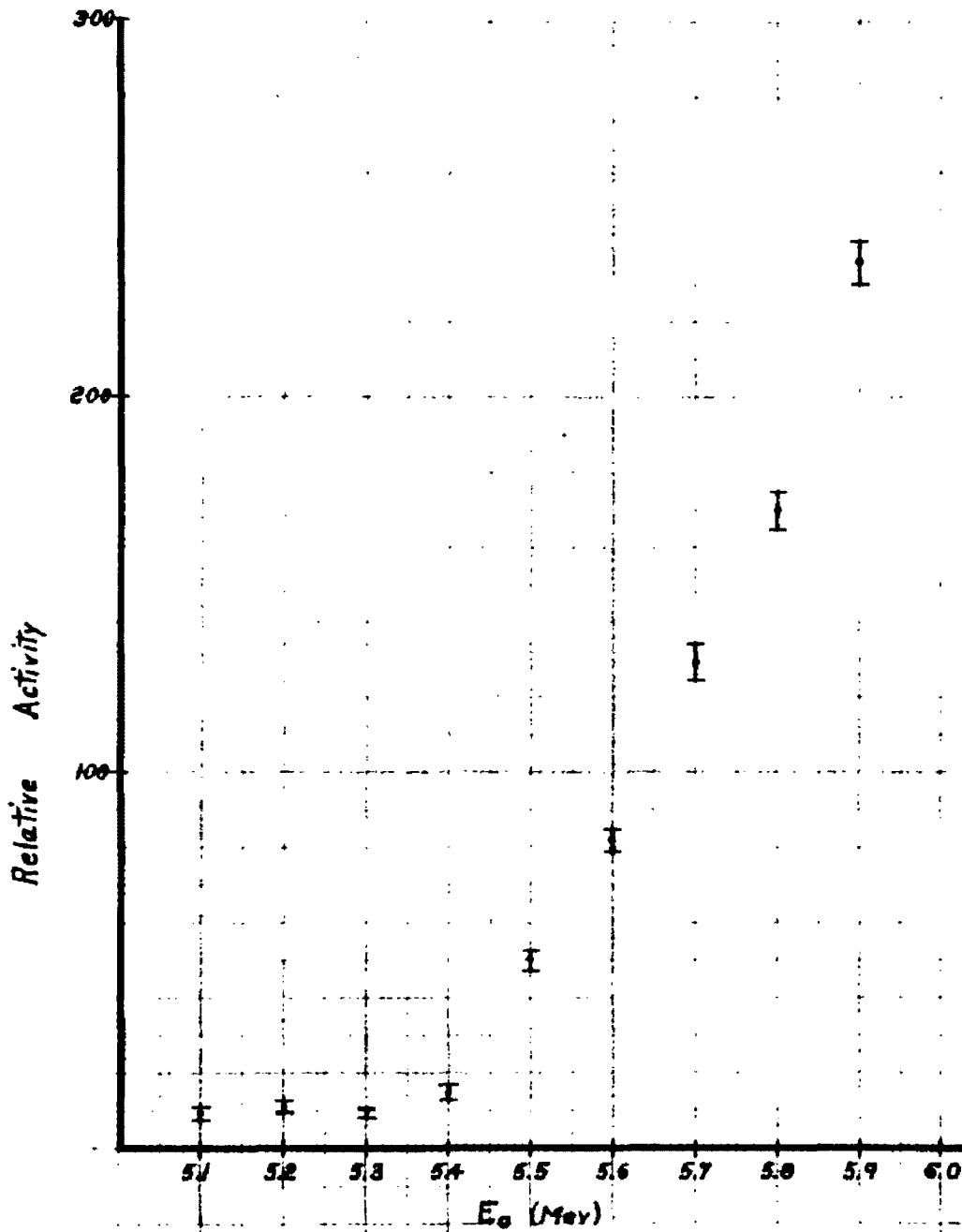


Fig 4 Activity of Fission Particles from U²³⁵ for Electron Energy E₀.

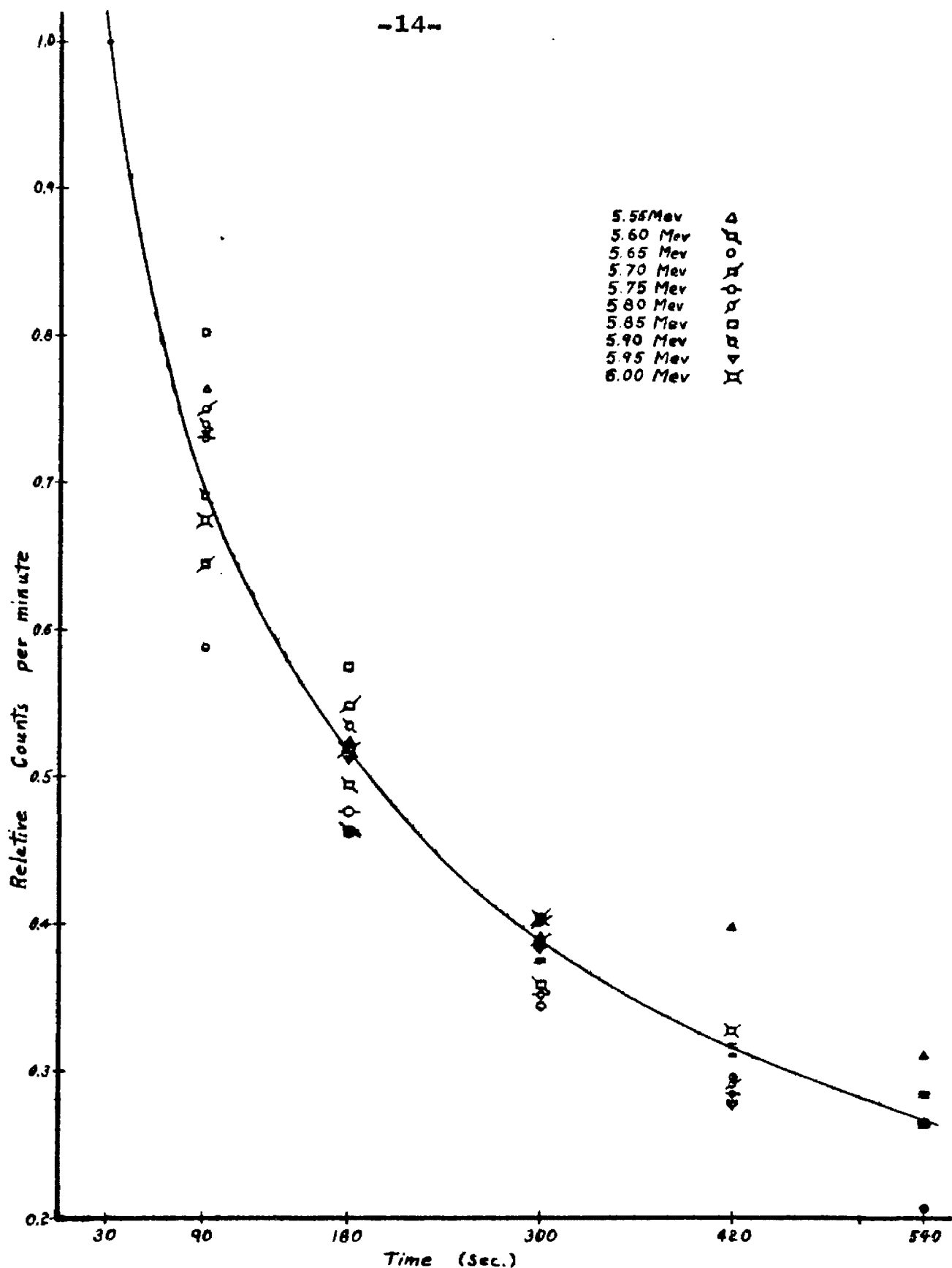


Fig. 5 Decrease in time of Activity of Fission Particles

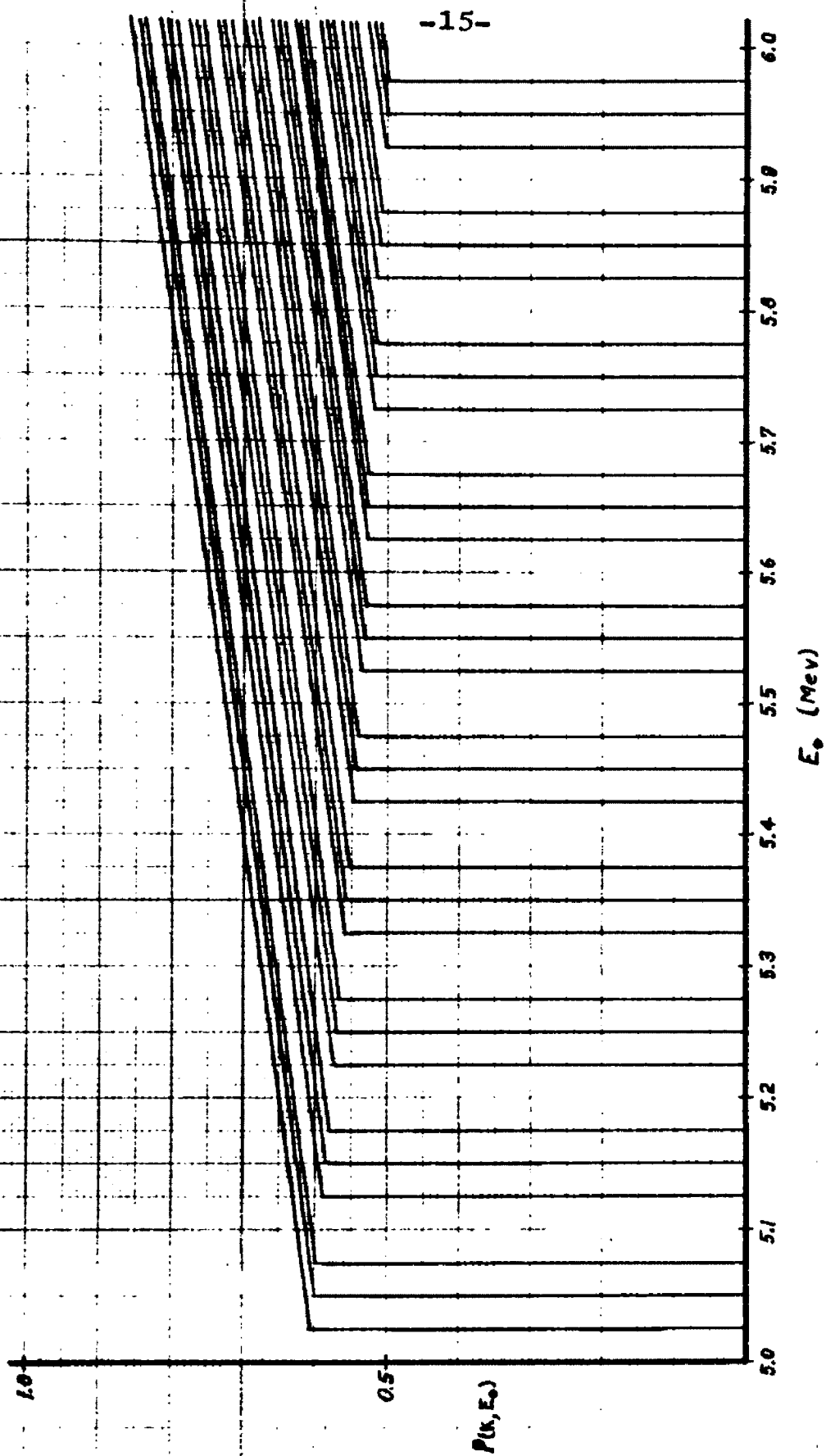


Fig. 6° $P(k, E_0)$ for Electron Energy E_0 .

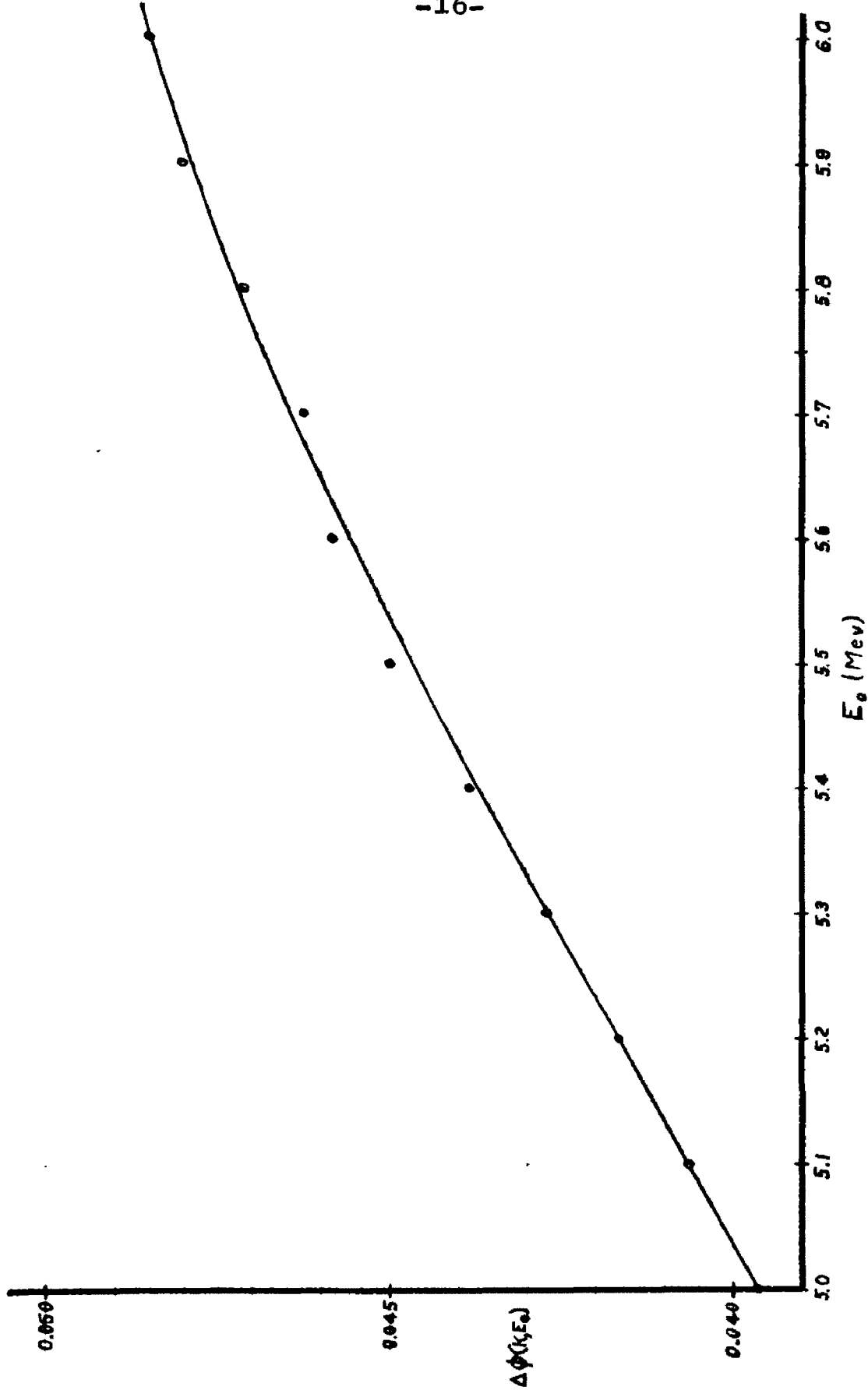


Fig. 7 $\Delta\phi(\kappa, E_0)$ for Electron Energy E_0 and $\epsilon = 0.1$ Mev.

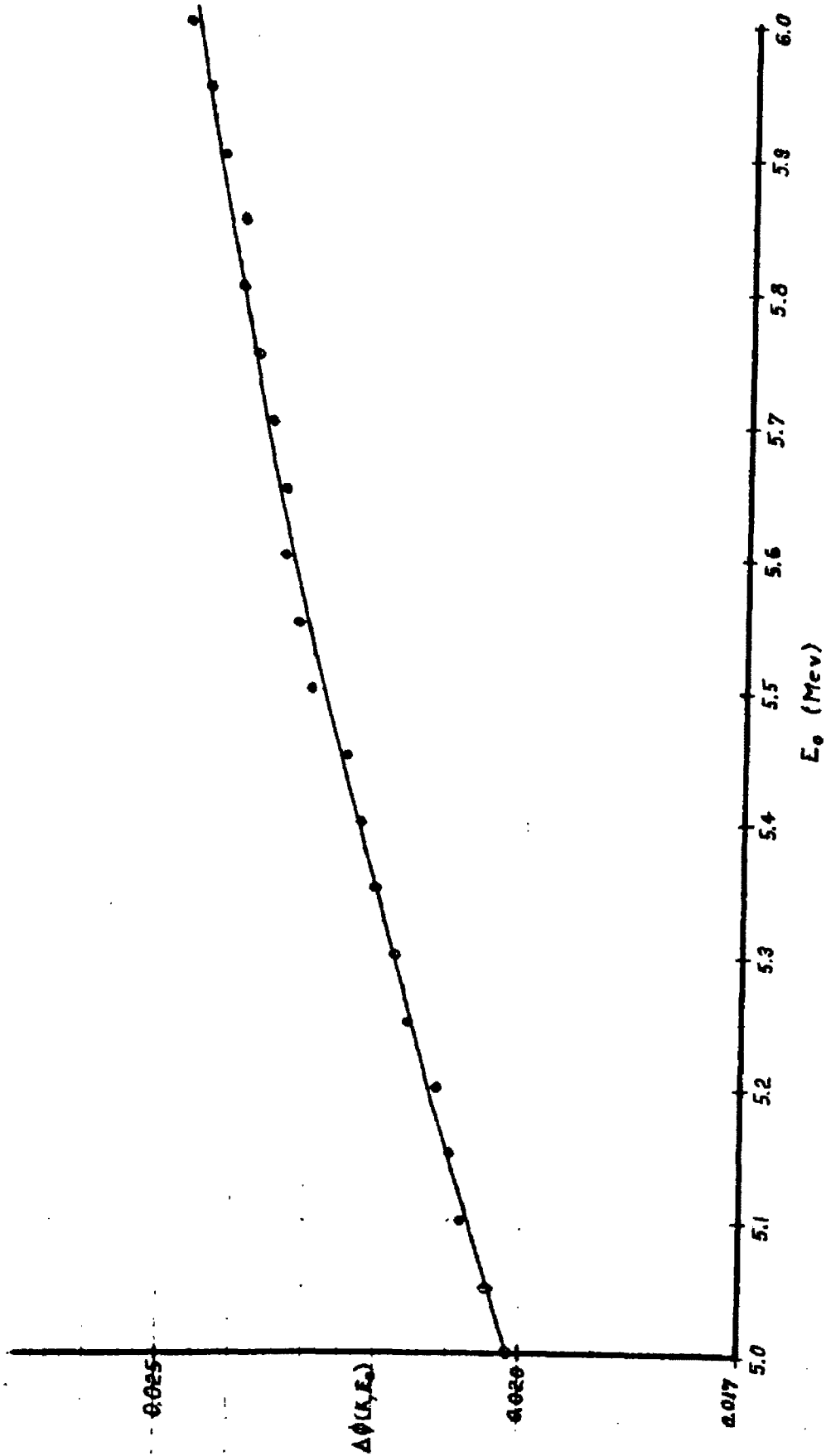


Fig. 8 $\Delta\phi(k, E_0)$ for Electron Energy E_0 and $\epsilon = 0.05$ MeV.

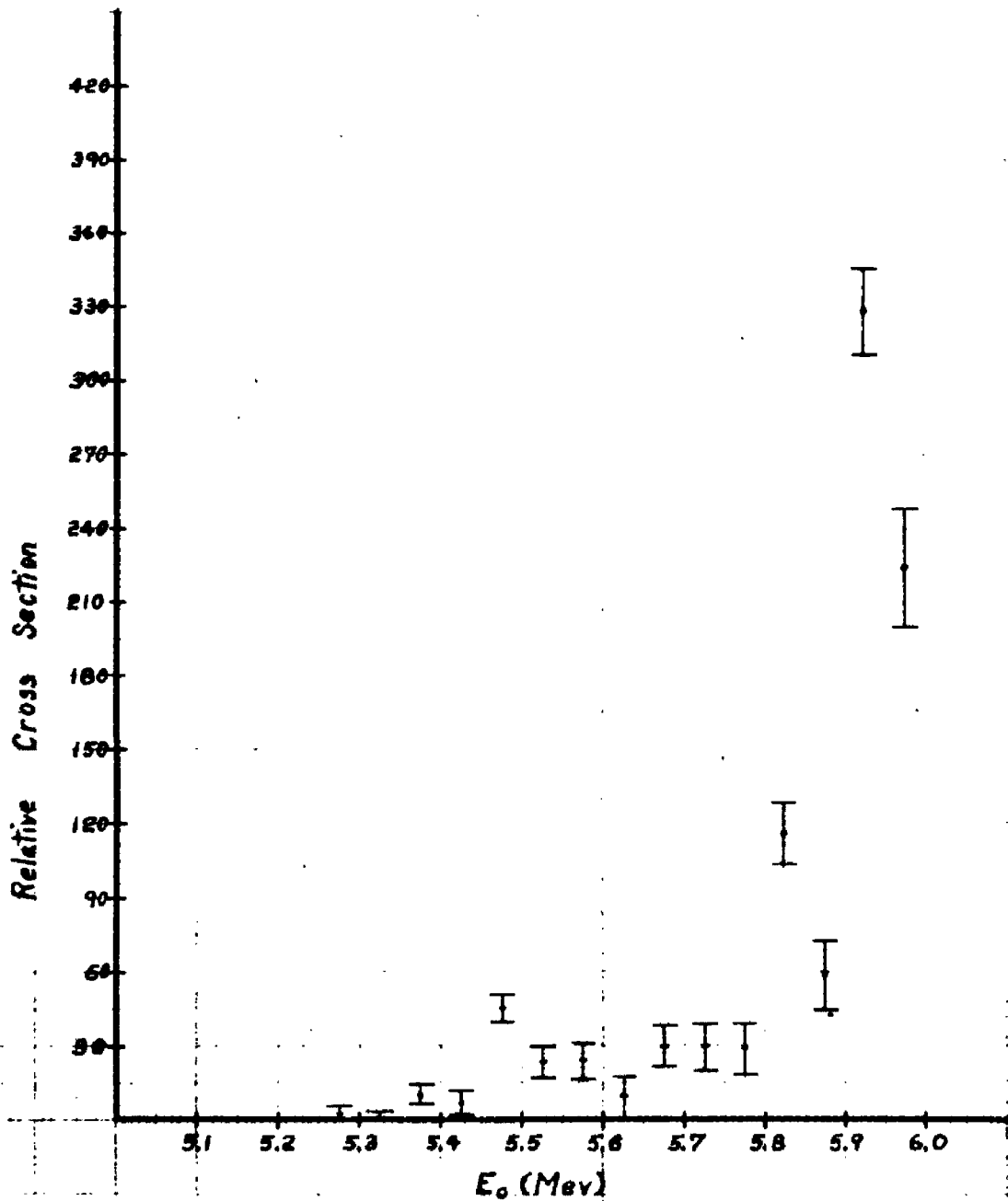


Fig. 9 $\sigma(E_0 - \frac{1}{2}\epsilon)$ of Th^{232} for Electron Energy E_0
and $\Delta = 0.05$ Mev
(Showing Standard Deviation)

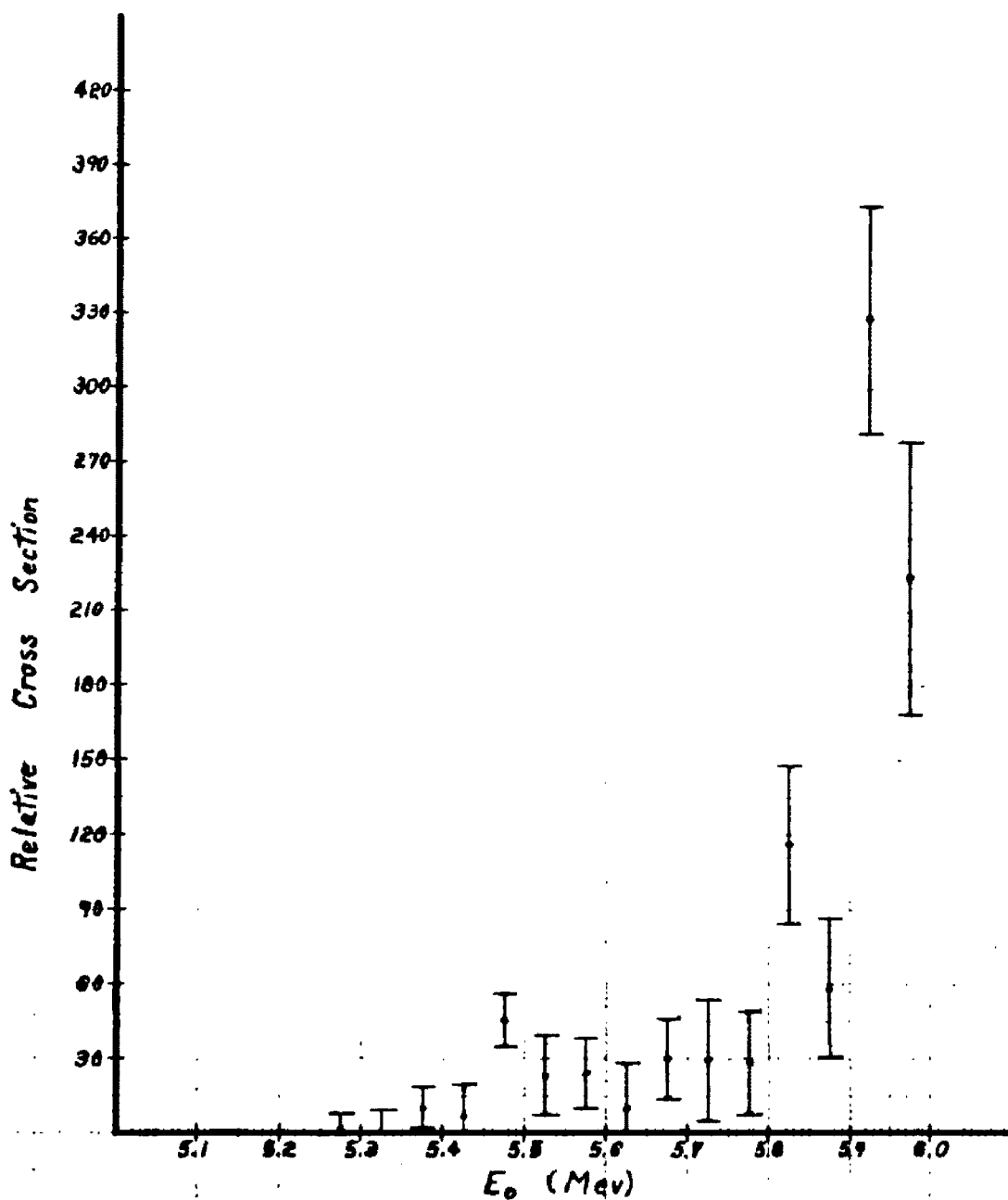


Fig. 10 $\bar{\sigma}(E_0 - \frac{1}{2}\epsilon)$ of Th^{232} for Electron Energy E_0
and $\epsilon = 0.05$ Mev
(Showing Total Error)

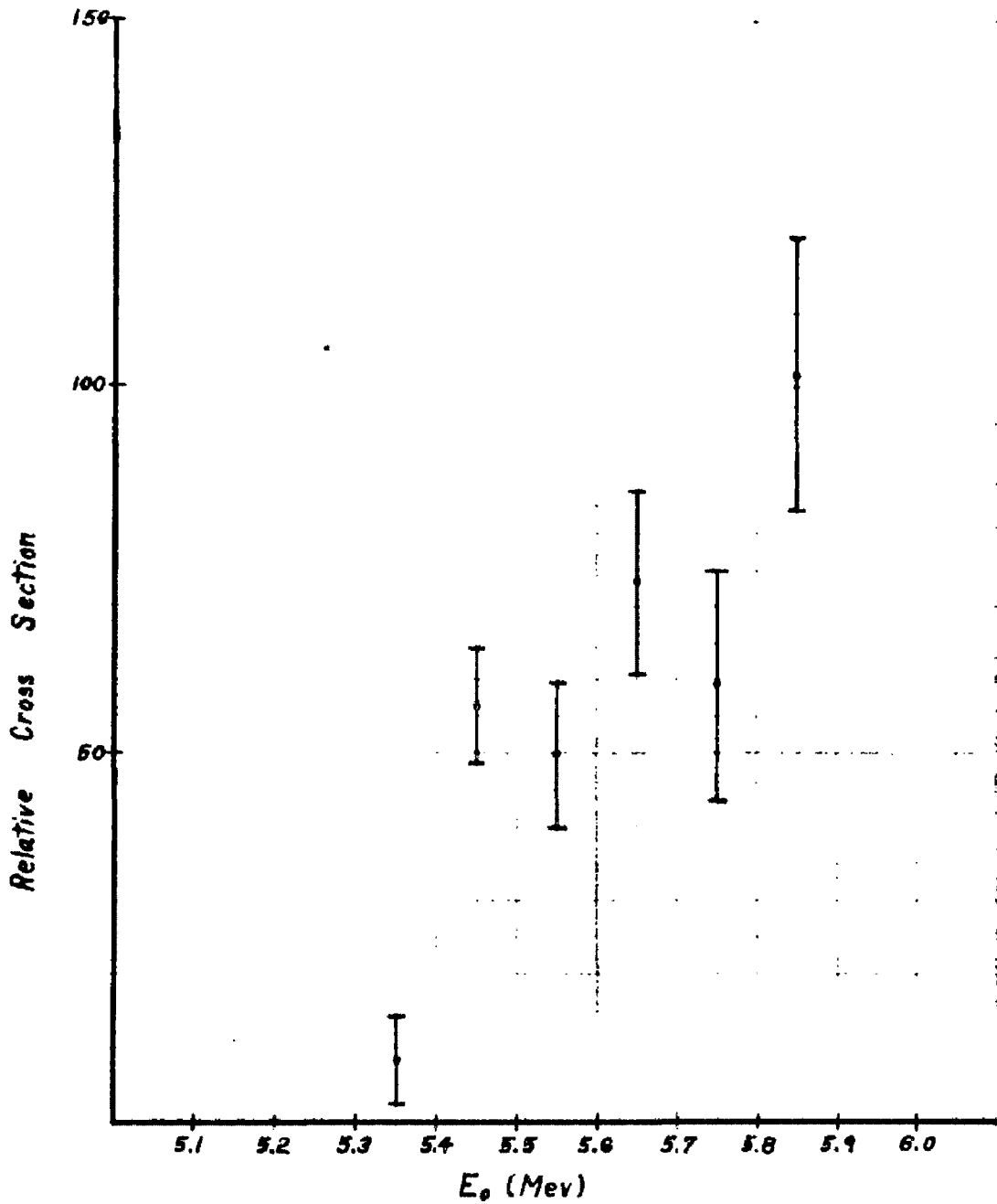


Fig. 11 $\bar{\sigma}(E_0 - \frac{1}{2}\epsilon)$ of U^{238} for Electron Energy E_0
and $\epsilon = 0.1$ Mev
(Showing Standard Deviation)

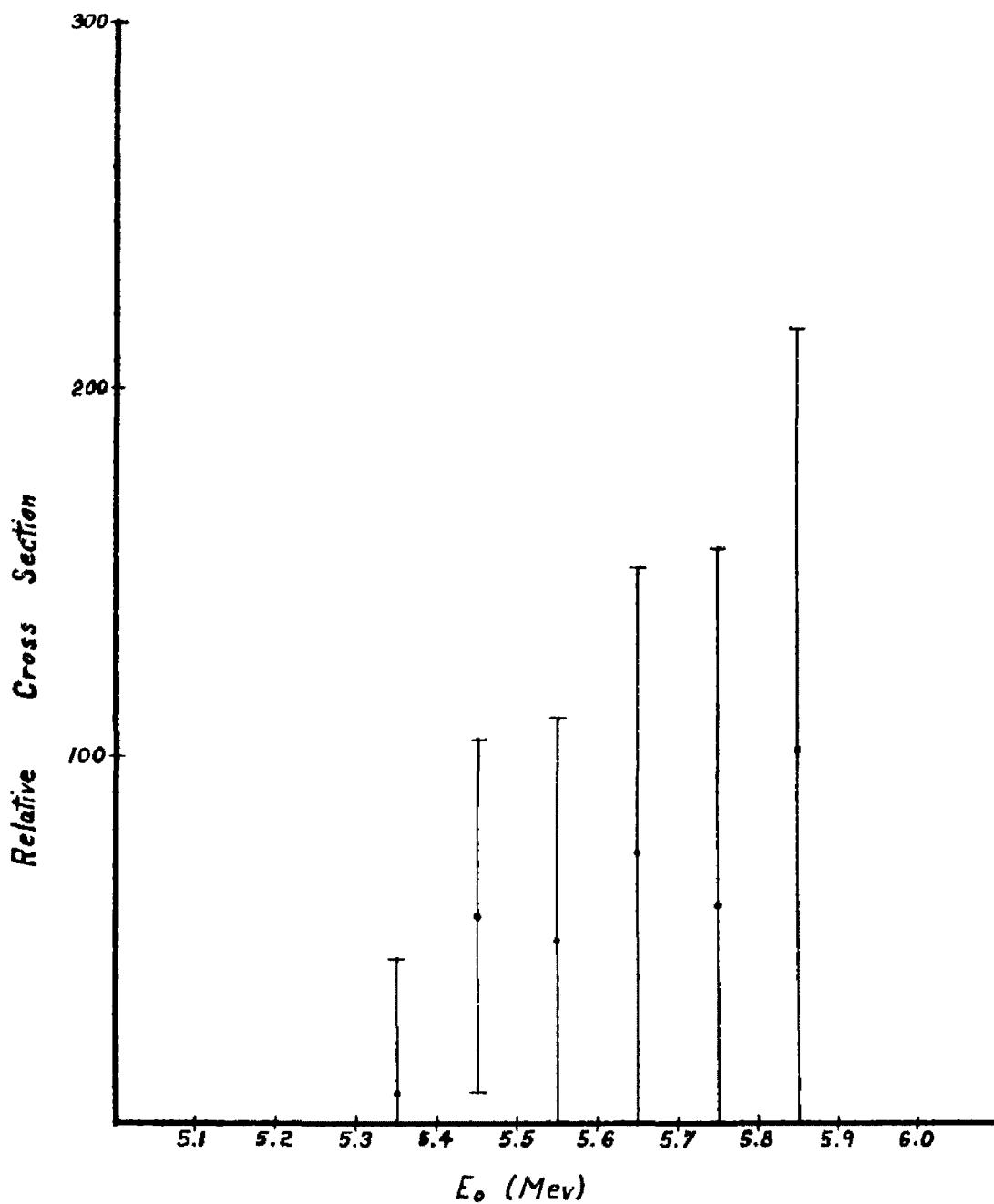


Fig. 12 $\bar{\sigma}(E_0 - \frac{1}{2}\epsilon)$ of U^{238} for Electron Energy E_0
and $\epsilon = 0.1$ Mev
(Showing Total Error)

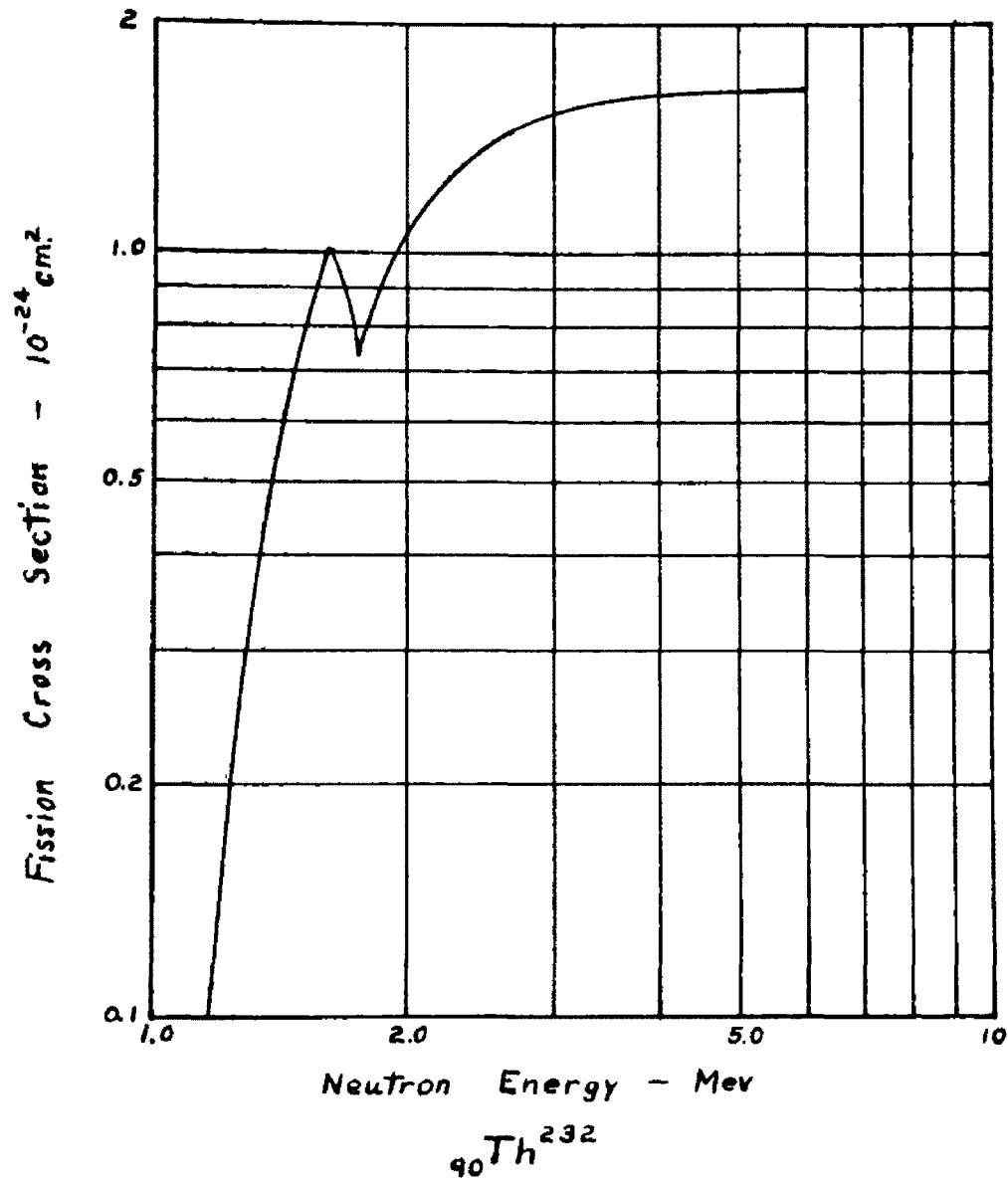
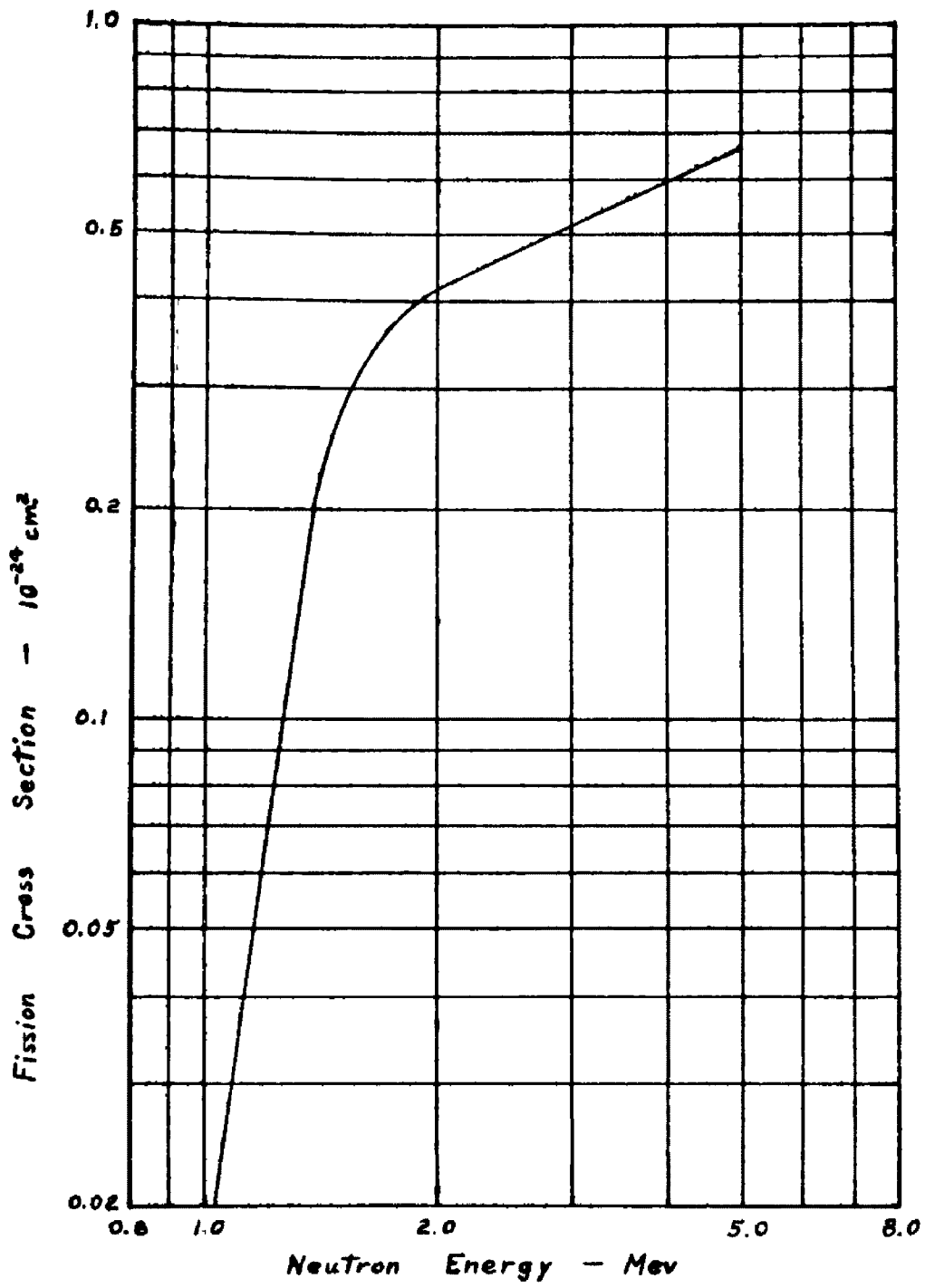


Fig. 13



^{92}U

Fig. 14

CONCLUSIONS

Fig. 5 shows that the activity of the fission fragments is effectively the same for the different energies. Thus the measurements indicate that the half lives of the fission fragments do not change appreciably for this energy range.

The activity measurement shows that Th^{232} does not have a uniform rate of increase above threshold. As the cross section computations are based on the rate of increase of activity, any change in this appears as a variation in the cross section. The fluctuation of the rate of increase in activity of Th^{232} shows up in this case as a peak between 5.4 and 5.5 Mev with a width of 50 Kev as indicated in Fig. 8. It is still evident when the total error is shown for the points (Fig. 9). Since this fluctuation is in close agreement with that reported in other work³ one is led to believe that there is a maximum in the Th^{232} cross section at 5.5 Mev.

In the case of U^{238} , further investigation needs to be done in order to demonstrate positively that its cross section differs from Th^{232} . If, as other work³ shows (and this research seems to indicate so), the two cross sections differ, then theory needs to be changed to account for the difference. In any case,

theory needs to be modified to explain the maximum in the Th^{232} cross section. It is also interesting to note that there is a sharp fluctuation in the neutron fission cross section² just above threshold for Th^{232} and none for uranium (Figs. 13 & 14). This variation may be due to a process similar to that occurring for the photofission cross section.

REFERENCES

- ¹Bohr, N. and Wheeler, J.A., Phys. Rev., 56, 426(1939).
- ²Hill, D.L. and Wheeler, J.A., Phys. Rev., 89, 1102 (1953).
- ³Katz, L., Baerg, A.P., and Brown, F., Proceedings of the International Conference on the Peaceful Uses of Atomic Energy, Geneva, 1958, P/200, Vol 15, p 180, United Nations, New York (1958).
- ⁴Segre, E., Experimental Nuclear Physics, John Wiley and Sons, Inc., New York, 1953, p 230.
- ⁵Jakobson, M.J., Phys. Rev., 123, 229 (1961).
- ⁶Katz, L. and Cameron, A.G., Can. J. Phys., 29, 518 (1951).
- ⁷Fano, U., Koch, H.W. and Motz, J.W., Phys. Rev., 112, 1679 (1958).
- ⁸Thies, H.H., Australian J. Phys., 14, 174 (1961).